ACS APPLIED MATERIALS & INTERFACES

Research Article

www.acsami.org

Hairy Polyelectrolyte Brushes-Grafted Thermosensitive Microgels as Artificial Synovial Fluid for Simultaneous Biomimetic Lubrication and Arthritis Treatment

Guoqiang Liu,[†,‡] Zhilu Liu,[†] Na Li,[§] Xiaolong Wang,*[,†] Feng Zhou,*[,†] and Weimin Liu[†]

[†]State Key Laboratory of Solid Lubrication, Lanzhou Institute of Chemical Physics, Chinese Academy of Sciences, Lanzhou 730000, P. R. China

[‡]Graduate School of Chinese Academy of Sciences, Beijing 100039, P. R. China

[§]School/Hospital of Stomatology, Lanzhou University, Lanzhou 730000, P. R. China

ABSTRACT: We report the fabrication of poly(3-sulfopropyl methacrylate potassium salt) (PSPMK) brushes grafted poly(*N*-isopropylacrylamide) (PNIPAAm) microgels and their potential as artificial synovial fluid for biomimetic aqueous lubrication and arthritis treatment. The negatively charged PSPMK brushes and thermosensitive PNIPAAm microgels play water-based hydration lubrication and temperature-triggered drug release, respectively. Under soft friction pairs, an ultralow coefficient of friction was achieved, while the hairy thermosensitive microgels showed a desirable temperature-triggered drugs release performance. Such a soft charged hairy microgel offers great possibility for designing intelligent synovial fluid. What is more, the combination of lubrication and drug loading capabilities enables the large clinical potential of novel soft hairy nanoparticles as synthetic joint lubricant fluid in arthritis treatment.

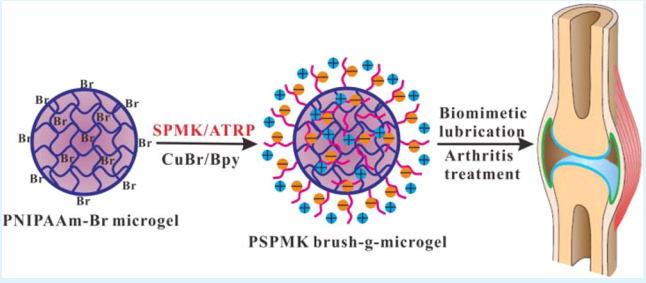

KEYWORDS: *hairy microgels, polyelectrolyte brushes, hydration lubrication, biomimetic synovial fluid, arthritis treatment*

1. INTRODUCTION

Biological water-based lubrication occurs between two parts of articular cartilage, which is the basic bearing biomaterial lining the bones of the joint. Because the biological surfaces display a fascinating low friction coefficient in the range 0.001−0.03 under changing conditions,[1] the lubrication of synovial joints is extremely efficient and undergoes more than 10^8 loading cycles over an 80-year lifespan.[2] Unfortunately, a failure of this lubrication leads to wear of the cartilage and thus to osteoarthritis.[3,4] To overcome the failure of joint lubrication, artificial joint replacement has been carried out, which, however, is always the last choice because of the great pain and the high cost for patients.[5] Accordingly, designing high-efficiency and biocompatible synthetic lubricant additives with medical treatment is believed to be a promising moderate approach to solving the troublesome problem, yet still a challenge.[6−8]

As we all know, the normal cartilage tissue is a kind of wet and soft multifunctional hydrogels in which a larger amount of water is interposed.[9] Similarly, synovial fluid is a clear, viscous liquid that acts a lubricant and shock absorber for the cartilage surfaces of the joint.[6] Synthetic bulk hydrogels for artificial cartilage tissue have been widely investigated,[10−13] while bioinspired nano/microgels for synthetic synovial fluid has rarely been reported, which may be another important strategy to biomimetic lubrication.

Water is the natural medium in the biological lubrication systems, but generally, water on its own is a poor lubricant because of low viscosity.[14] Fortunately, in the body, the poor lubrication of water can be overcome by biological lubricant additives. For example, as a biological polyelectrolyte, the glycoproteins play a key role in the articular cartilage lubrication. This glycoprotein shows a bottle-brush architecture, in which large numbers of sugar chains are grafted along a protein backbone.[15] Inspired by this biopolymer, biomimetic bottle-brush polymer have been synthesized and exhibits low friction.[16] The hydrophilic polymer brushes can achieve excellent hydration lubrication by forming hydrated layer surrounding charges in aqueous media.[17,18]

Microgels are cross-linked polymeric micro/nanoparticles with network structures, and the interstitial space of the network can be filled with fluid.[19−21] Importantly, microgels with viscoelastic property are capable of undergoing large deformation in response to environmental change.[22] In particular, stimuli-responsive microgels, with faster response to external stimuli and better dispersion in aqueous media compared to bulk hydrogels,[23−25] is believed to be a promising candidate for low-friction intelligent biomimetic lubricant as the

Received: September 4, 2014
Accepted: October 27, 2014
Published: October 27, 2014

substitute of synovial fluid.[26−28] Importantly, the microgels can load drug to achieve a stimuli-triggered release in the lesion site, which may be an effective approach to treat arthritis. Moreover, it is well-known that the main components of synovial fluid are hyaluronan, aggrecan, and glycoproteins lubricin, which all belong to biopolyelectrolytes.[28] Therefore, presently, inspired by the biological systems, the synergistic combination of polymer brushes and soft microgels for water lubrication may be a promising strategy for simultaneous biomimetic lubrication and arthritis treatment.

In our study, soft hairy polyelectrolyte brushes grafted microgels were designed to mimic the synovial fluid and achieve the possibility of arthritis treatment. The hairy structured microgels fix the macro-irons on the polymer chains and localize the microcounter ions in the charged polymer network. In aqueous media, the hydrated layer can be formed surrounding the negatively charged polymer brushes and achieve effective hydration lubrication.[29,30] In addition, compared with polymer brush-functionalized inorganic nanoparticles, soft hairy microgels possess flexible deformability and viscoelasticity and can better adapt to environmental change without being destroyed.[31,32]

Herein, we address the biomimetic synovial fluid using the negatively charged poly(3-sulfopropyl methacrylate potassium salt) (PSPMK) brushes grafted poly(*N*-isopropylacrylamide) (PNIPAAm) microgels (SB-*g*-NBrMGs). The PNIPAAm microgels were employed as the cores of SB-*g*-NBrMGs to provide the thermosensitive drug release, while the PSPMK brushes grafted to the PNIPAAm cores endow the microgels with biomimetic polyelectrolyte structure to achieve good hydration lubrication. The hairy microgels were found to possess excellent tribological properties and temperature-triggered drug release performance. Especially, the ultralow friction coefficient still can be obtained at higher temperature, which cannot be achieved by the traditional PNIPAAm microgels. It is beneficial for in vivo application that the good lubricating effect can be maintained over a wide temperature range. The design of hairy charged polymer brushes-grafted thermoresponsive microgels offers immense potentials of soft hairy microgels as intelligent synovial fluid for high-efficiency joint lubrication together with the possibility of arthritis treatment in the clinical medicine.

2. EXPERIMENTAL SECTION

2.1. Materials. 2-Hydroxyethyl methacrylate (HEMA, 99%), 2-bromoisobutyryl bromide (98%), *N*-isopropylacrylamide (NIPAAm, 99%), N,N′-methylenebis(acrylamide) (MBA, 98%), triethylamine (99%), and aspirin (98%) were purchased from J&K Chemical Ltd. and used as received. Potassium persulfate (KPS) and 2,2-Azobis-(isobutyronitrile) (AIBN, AR) bought from Sinopharm Chemical Reagent Co. Ltd., China, were both purified by recrystallization in ethanol before use. Dichloromethane (Tianjin Chemical Reagents Corp.) was dried over CaH_2 before use. 3-Sulfopropyl methacrylate potassium salt (98%, SPMK), 2,2′-bipyridine (Bpy, 99%), and copper(I) bromide (CuBr) were purchased from TCI Co., Ltd. CuBr was purified by stirring overnight in acetic acid. 3-(Trimethoxysilyl)propyl methacrylate (MPS, 98%) was purchased from Sigma-Aldrich and used without further purification. 3-(Trichlorosilyl)propyl-2-bromo-2-methylpropanoate (SI-ATRP initiator) was synthesized in our lab. After filtration, it was washed with ethanol and diethyl ether and then dried in vacuum. THF, *n*-hexane, and methanol were used as received. Deionized water was applied for all polymerization and treatment processes.

2.2. Synthesis of 2-(2-Bromoisobutyryloxy)ethyl Methacrylate (HEMA-Br). 2-Bromoisobutyryl bromide (1.85 mL, 15.0 mmol) was added dropwise to a solution of HEMA (1.50 mL, 12.4 mmol) and triethylamine (4.17 mL, 30.0 mmol) in 50 mL of dichloromethane at 0 °C under argon atmosphere. The solution was stirred at 0 °C for 2 h and then for another 12 h at 25 °C to complete the reaction. The white precipitate was filtered and washed with ethyl acetate twice. The organic phases were combined, washed with water several times, and dried with magnesium sulfate ($MgSO_4$). After the solvent was evaporated, the crude product was purified by column chromatography, resulting in a pale yellow liquid, which was well-defined by ^1H NMR.

2.3. Synthesis of Thermoresponsive PNIPAAm-Br Microgels. The thermosensitive PNIPAAm microgels with ATRP-Br initiator (PNIPAAm-Br microgels) were prepared by emulsifier-free emulsion polymerization. The typical procedures are described in the following. NIPAAm (1.0 g), HEMA-Br (0.05 g), cross-linking agent MBA (0.032 g, 3.0 wt %), and H_2O/ethanol (v/v = 10:1, 100 mL) were added to a 250 mL round-bottom flask with a mechanical stirrer, condenser, and nitrogen inlet. After dispersing sufficiently with a fine stream of nitrogen at room temperature for 30 min, KPS (0.032 g, 3.0 wt %) was added to initiate polymerization. The continuous polymerization reaction was conducted for 8 h at 75 °C. After polymerization, the product was purified in a dialysis tube (molecular weight cutoff at 12 kDa, Sigma-Aldrich) with 1000 mL of deionized water for 72 h. The deionized water was exchanged at intervals of 12 h.

2.4. Synthesis of PSPMK Brushes-Grafted PNIPAAm Microgels. The PSPMK brushes-grafted PNIPAAm microgels (SB-*g*-NBrMGs) were synthesized by surface-initiated atom transfer radical polymerization (SI-ATRP). Typically, the initiator-immobilized PNIPAAm-Br microgel aqueous suspension (8 mL), SPMK (1.5 g), and MeOH (2.0 mL) were charged into a polymerization tube. The microgels were dispersed ultrasonically for 5 min. The dispersion was deoxygenated by bubbling nitrogen gas at room temperature for 30 min, then 2,2′-bipyridyl (0.0625 g, 0.4 mmol) and CuBr (0.0287 g, 0.2 mmol) were added into the tube quickly. The polymerization was conducted at room temperature under N_2 protection for 2 h. After polymerization, the product was purified in a dialysis tube (molecular weight cutoff at 12 kDa, Sigma-Aldrich) with 1000 mL of deionized water for 72 h and it was exchanged at intervals of 12 h.

2.5. Synthesis of Brush-Like Polymer PSPMK Brushes-*g*-PNIPAAm. The brush-like polymer PSPMK brushes-*g*-PNIPAAm (SB-*g*-PNIPAAm) was synthesized with PNIPAAm as the backbone and PSPMK brushes as the grafted chains. First, the PNIPAAm backbone containing ATRP-Br was prepared through radical copolymerization of NIPAAm and HEMA-Br in THF. Typically, NIPAAm (1.0), HEMA-Br (0.05 g), AIBN (0.005 g), and THF (50 mL) were put into a 100 mL round-bottom flask with a magnetic stirrer. The flask was then deoxygenated under reduced pressure and backfilled with nitrogen several times. The reaction was carried out at 70 °C for 24 h. The obtained sample was purified through dissolution/precipitation in hexane several times. Second, the PSPMK brushes were grafted from the PNIPAAm backbone through ATRP. Typically, the PNIPAAm-Br and SPMK was first dispersed in methanol/H_2O (v/v = 2:1), and the polymerization tube was deoxygenated by bubbling nitrogen gas at room temperature for 30 min. Afterward, 2,2′-bipyridyl (0.0625 g) and CuBr (0.0287 g) were added into the tube quickly. The polymerization was conducted at room temperature under N_2 protection for 2 h. The sample was obtained through vacuum distillation and then purified through dissolution/precipitation in THF/hexane several times.

2.6. Fabrication of PDMS Hemisphere and Modification with PSPMK Brushes or PNIPAAm Hydrogel. The PDMS ball was prepared in a hemispheres mold using commercial silicone elastomer kit (SYLGARD 184 silicone elastomer). The base and curing agents of SYLGARD 184 elastomer kit were mixed at 10:1 ratio (by weight).[33,34] The mixtures were transferred into the mold after removing bubbles under gentle vacuum and then incubated in an oven (80 °C) for 24 h. Prior to friction measurement, the PDMS hemisphere was coated with PSPMK brushes or PNIPAAm hydrogel shell.

2.6.1. Modification with PSPMK Brushes. Plasma oxidized PDMS hemisphere and a vial containing 10 μL of 3-(trichlorosilyl)propyl 2-bromo-2-methylpropanoate were put into a vacuum desiccator. The chamber is pumped down to <1 mbar, and left under vacuum for 30 min. This process was cycled for 3 times. Then, PSPMK brushes were grafted onto the ATRP initiator modified PDMS hemisphere through SI-ATRP. Briefly, the initiator modified PDMS hemisphere, SPMK (1.5 g), 2,2′-bipyridyl (0.0628 g), 9 mL of methanol/H_2O (v/v = 2:1) were added into a polymerization tube. The reaction system was deoxygenated by bubbling nitrogen gas for 30 min. Then, CuBr (0.0287 g) were added into the tube quickly. The polymerization was conducted under N_2 protection for 2 h. The obtained PSPMK brushes-grafted-PDMS hemisphere was washed with deionized water for further friction test.

2.6.2. Modification with PNIPAAm Hydrogel. Plasma oxidized PDMS hemisphere was immersed into 50 mL of ethanol/H_2O (v/v = 4:1) solution containing 1.5 mL of $NH_3{\cdot}H_2O$ and 0.2 g of 3-(trimethoxysilyl)propyl methacrylate for 24 h. The PDMS hemisphere with C═C bonds was obtained and washed with deionized water. Then, the PDMS hemisphere was coated with PNIPAAm hydrogel shell through distillation−precipitation polymerization. Typically, MPS modified PDMS hemisphere, 0.5 g of NIPAM, 30 mg of MBA, and 10 mg of AIBN were dispersed in 20 mL acetonitrile in a dried 50 mL single-necked flask. The mixture was heated to the boiling state, and the reaction was ended after about 10 mL of acetonitrile was distilled from the flask. The obtained PDMS hemisphere with PNIPAAm hydrogel shell was washed with deionized water for further friction test.

2.7. In Vitro Cytotoxicity Test. The in vitro cytotoxicity of SB-*g*-NBrMGs was evaluated by standard MTT assay using the Hela cells. The Hela cells were seeded on 96-well plates at a density of 1×10^4 cells per well and cultured in a standard cell culture medium for 24 h. Then, the cells were exposed to SB-*g*-NBrMGs with different concentrations and incubated for 24 h. Afterward, the supernatants were removed and cells were washed with PBS solution. The MTT solution (50 μL, 0.5 mg/mL) were added to each well. After incubation for another 4 h, the culture medium was removed. 100 μL of DMSO was added into each well and dissolved the precipitates. The absorbance of theses sample was measured at 570 nm on a microplate reader. The cell viability was determined by the following equation: cell viability (%) = $OD_{treated}/OD_{control} \times 100$, where $OD_{treated}$ was obtained from the cells treated with SB-*g*-NBrMGs, and $OD_{control}$ was obtained from the untreated cells and defined as 100% viability.

2.8. Fabrication of Drug-Loaded SB-*g*-NBrMGs Microgels. Before the drug-release experiment, the calibration curve was prepared first. The absorbance of aspirin PBS buffer solutions with different concentrations was measured on the UV−vis spectrophotometer at 296 nm and calibration graph was constructed. The concentration of the aspirin in the sample solution was read from the graph as the concentration corresponding to the absorbance of the solution.

Aspirin was added to SB-*g*-NBrMGs suspension in a flask and oscillated at room temperature for 48 h. The aspirin loaded SB-*g*-NBrMGs were separated by centrifugation, washed with water several times, and dispersed in PBS buffer solutions. The amount of aspirin encapsulated by microgels was measured by determining the concentration difference in the loading medium before and after loading. The amount of aspirin was analyzed using UV−visible spectrophotometer at a wavelength of 296 nm.[35] The drug loading capacity (LC) and encapsulation efficiency (EE) were calculated with the following formulas, respectively.

$$\text{LC}\ (\%) = \frac{\text{amount of loaded aspirin}}{\text{amount of aspirin loaded SB-}g\text{-NBrMGs}} \times 100$$

$$\text{EE}\ (\%) = \frac{\text{amount of loaded aspirin}}{\text{total amount of added aspirin}} \times 100$$

2.9. In Vitro Drug Release. The in vitro release behavior of aspirin loaded SB-*g*-NBrMGs at different temperature was monitored by the dialysis tube diffusion technique.[36] The aspirin loaded SB-*g*-NBrMGs were enveloped into a dialysis tube (molecular weight cutoff = 8000−10000). Then, the tube was dialyzed against the 500 mL of phosphate buffer solution (pH = 7.4) in a separate beaker. After a predetermined period, certain amount of the release medium was taken out and replaced by the same amount of fresh PBS solution to maintain the volume of the medium constant. The released aspirin amount was determined by UV analysis with a calibration curve as described above. The release percent of aspirin was calculated by the equation:

$$\text{Drug release}\ (\%) = \frac{\text{Mt}}{\text{Ma}} 100$$

Here, Mt is the amount of aspirin released from the as-prepared nanoparticles at time *t*, while Ma is the total amount of aspirin—the encapsulated amount. Release experiments were conducted until the concentration of the solution stopped changing significantly. Each measurement was repeated three times and the average value was calculated.

2.10. Characterization. Scanning electron microscopy (SEM) images were obtained from a JSM-6701F (JEOL, Japan) scanning electron microscope with a field emission gun operating at 200 kV. The elemental composition was evaluated using energy-dispersive X-ray spectroscopy (EDXS, attached to the SEM apparatus).

Fourier transform infrared (FT-IR) spectra were determined on a Nicolet iS10 (Thermo Scientific, U.S.A.) FT-IR spectrometer. ^{1}H NMR spectrum was recorded on a UNITY INOVA 600-MHz spectrometer (Varian, U.S.A.). Thermogravimetric analysis (TGA) measurements were performed on a STA 449C Jupiter simultaneous TG-DSC instrument from ambient temperatures to approximately 800 °C in an air atmosphere.

Hydrodynamic diameters (D_h) and ζ-potential were measured by dynamic light scattering technique (DLS) using a particle size analyzer (Zetasizer Nano ZS, Malvern Instruments, U.K.) equipped with a 632.8 nm He−Ne laser. The swelling ratio (SR) was determined by the following equation: $SR = V_{swollen}/V_{collapse} = (D_{25}/D_{45})^3$, where $V_{swollen}$ and $V_{collapse}$ were the volumes of microgel particles in the swollen state (25 °C) and collapse state (45 °C), respectively. D_{25} and D_{45} were the mean hydrodynamic diameters of the microgels at 25 and 45 °C, respectively.

The rheological behavior was investigated by RS6000 Rheometer (Germany) using a parallel-plate geometry (diameter, 35 mm; gap, 1 mm) at 25 °C. The concentration of microgel suspension was 1.0 wt %, and the amount of the suspension dropped on the plate was 1.0 mL. In rheology, tan δ was defined as "dissipation factor", where tan δ = G'' (loss modulus)/G' (storage modulus), which indicates the capability of dissipating energy away from the loadbearing surfaces.

The frictional tests were carried out in a ball-on-block configuration on 14-FW reciprocating friction tester (Japan, HEIDON Co., Ltd.) equipped with a thermostatically controlled platform. The contact between the frictional pair was achieved by pressing the upper running ball against the lower stationary disk which was driven to reciprocate at a given sliding rate (100 mm/min) and normal load (from 1 to 10 N) for 100 cycles. The distance of one sliding cycle was 30 mm. The upper ball is elastomeric poly(dimethylsiloxane) (PDMS) hemisphere with a diameter of 10 mm. The lower stationary disk was silica wafer (100 orientation, one side polished), which was treated in an oxygen plasma chamber (Diener electronic, Germany) at <200 mTorr and 100 W for 5 min. The friction test was repeated three times, and an average coefficient of friction was recorded.

The UV-spectra were recorded on a Cary 60 UV−vis spectrophotometer (Agilent Technologies, Palo Alto, CA). The physisorption in swollen and collapsed states on SiO_2-coated quartz crystal substrate was studied by a quartz crystal microbalance (E4, Q-Sense, Gothenburg, Sweden) with dissipation (QCM-D) monitoring technique. Because the resonant frequency shift (Δf) has a negative correlation with the adsorption amount on quartz crystal, Δ*f* referred to pure water was used to qualitatively present the adsorption amount of microgels on quartz crystal surface. The experiment was performed at 25 and 45 °C, respectively. X-ray photoelectron spectrometer (XPS) was employed to characterize the elemental composition of surface

Scheme 1. Schematic Illustration for the Fabrication of PSPMK Brushes-Grafted PNIPAAm Microgels, the Drug Loading and Release of the Hairy Spherical Microgels, and the Tribological Process of the Polyelectrolyte Microgels As a Biomimetic Synovial Fluid[a]

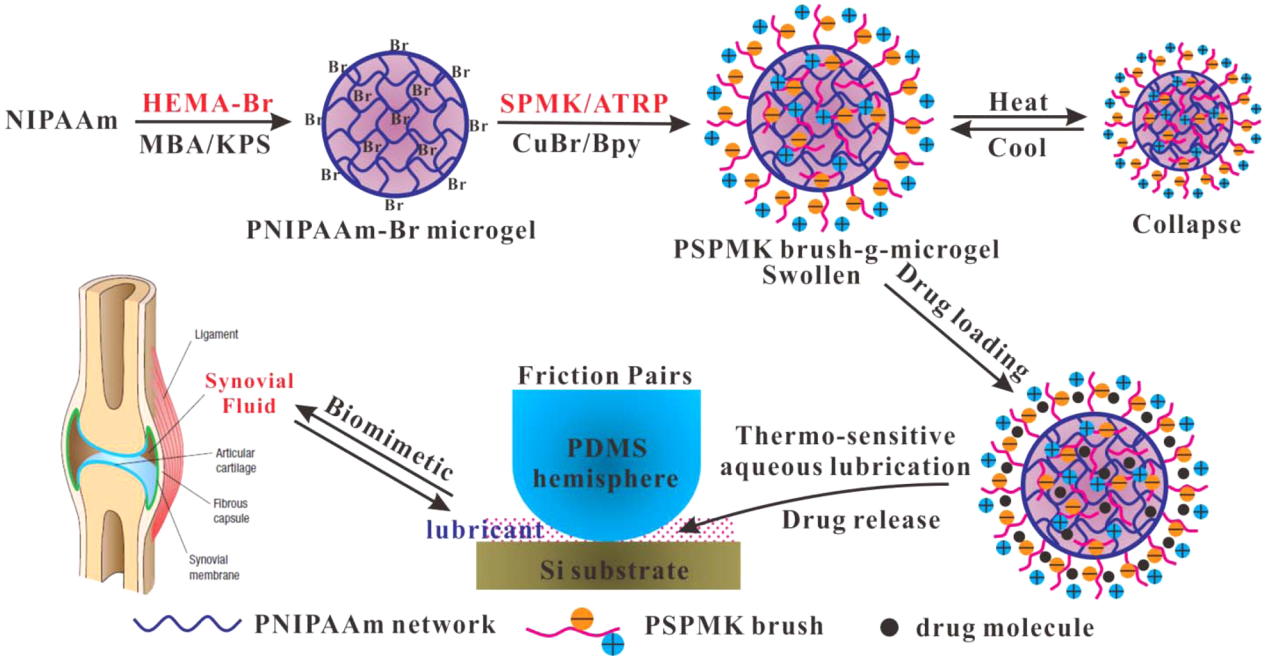

[a]The simulated joint diagram derives from the ref 40. (Lori Setton *Nat. Mater.* **2008**).[40]

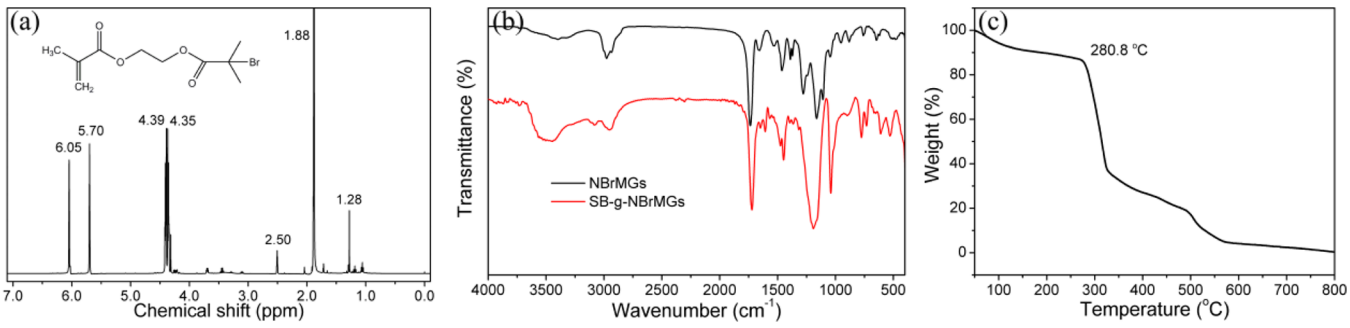

Figure 1. (a) ^{1}H NMR of HEMA-Br, (b) FT-IR of NBrMGs and SB-*g*-NBrMGs, and (c) TGA curve of SB-*g*-NBrMGs.

adsorption layer. The binding energy was referenced to the C 1s of contaminated carbon at 284.8 eV.

3. RESULTS AND DISCUSSION

In our work, negatively charged poly(3-sulfopropyl methacrylate potassium salt) (PSPMK) brushes were employed as the out-layer of designed hairy microgels to provide hydration lubrication. PSPMK brushes have a strong hydration capability and can be fully extended in aqueous media,[37,38] and furthermore, the polyelectrolytes surrounding the micro/nanoparticles play an important role in colloid stabilization because of electrostatic and steric interactions.[39] The schematic illustration of the fabrication of PSPMK brushes-grafted PNIPAAm microgels, the drug loading and release of the hairy spherical microgels, and the tribological process of the polyelectrolyte microgels as a biomimetic synovial fluid are shown in Scheme 1.

3.1. Chemical Structure Analysis. First, the monomer containing ATRP initiator HEMA-Br was synthesized according to the previous method.[41−43] Second, the thermoresponsive PNIPAAm-Br microgels (NBrMGs) were prepared through the copolymerization of NIPAAm and HEMA-Br by emulsifier-free emulsion polymerization. Finally, the PSPMK brushes-grafted PNIPAAm microgels (SB-*g*-NBrMGs) were synthesized by surface-initiated atom transfer radical polymerization (SI-ATRP).

The HEMA-Br was synthesized through the esterification reaction of HEMA and 2-Bromoisobutyryl bromide. The 1H NMR of HEMA-Br is shown in Figure 1a. The peaks were assigned as follows: δ = 6.05 (s, 1H, CHH=C(CH_3)—), 5.70 (s, 1H, CHH=C(CH_3)—), 4.39−4.35 (m, 2H, —CH_2CH_2—), 1.88 (s, 6H, ($CH3)_2$CBr), 1.28 (s, 3H, CH_3C=CH_2). In addition, the peak at 2.50 ppm was assigned to DMSO-d_6.

The chemical composition of NBrMGs and SB-*g*-NBrMGs were characterized using Fourier transform infrared (FTIR) spectroscopy. Figure 1b depicts the FTIR spectra of NBrMGs and SB-*g*-NBrMGs. For NBrMGs, the wide absorption band at 3650−3250 cm^{-1} and the absorption peak at 1658 cm^{-1} are associated with N−H groups and amide carbonyl in NIPAAm, respectively. The double peaks at 1391 and 1370 cm^{-1} are assigned to the coupling vibration split absorption of the two

dx.doi.org/10.1021/am506026e | *ACS Appl. Mater. Interfaces* 2014, 6, 20452−20463

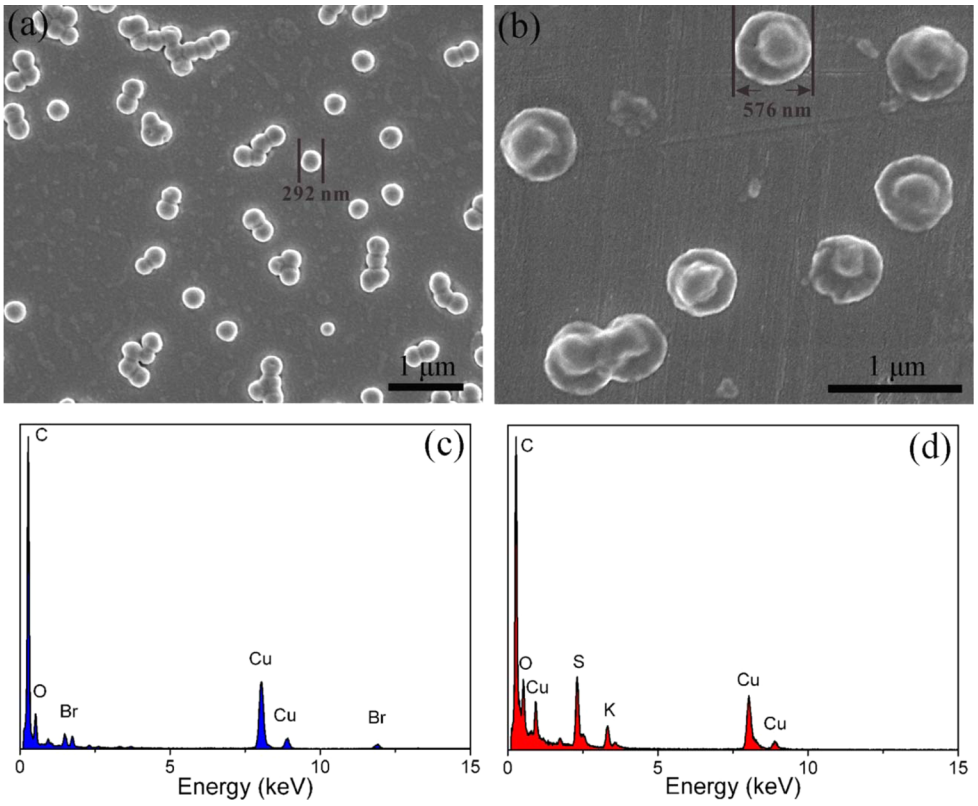

Figure 2. SEM images of (a) NBrMGs and (b) SB-*g*-NBrMGs; EDXS spectra of (c) NBrMGs and (d) SB-*g*-NBrMGs.

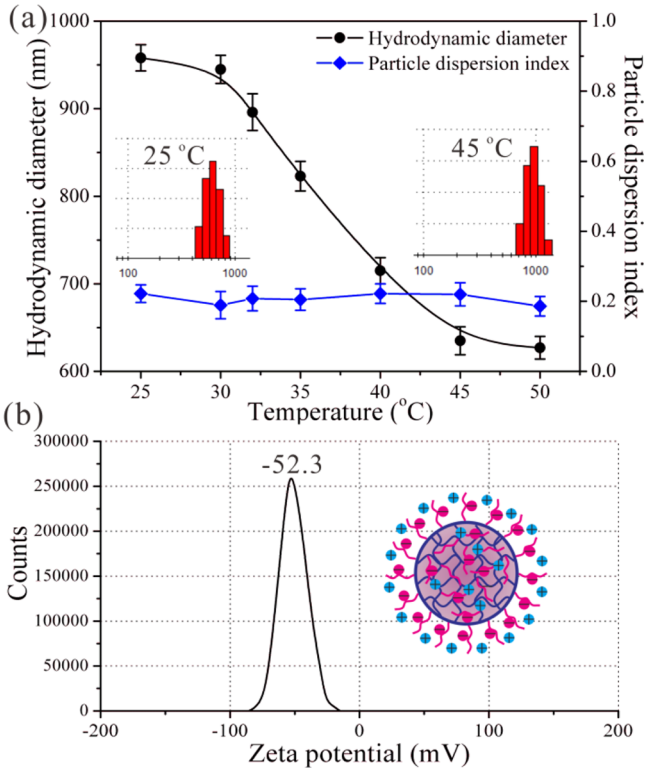

Figure 3. (a) Hydrodynamic diameter (D_h) and (b) the corresponding ζ-potential distributions of SB-*g*-NBrMGs in aqueous media.

methyl groups in $-CH(CH_3)_2$ of NIPAAm. The peak at 1731 cm^{-1} corresponds to the ester carbonyl groups of HEMA-Br. These peaks indicate a successful copolymerization of NIPAAm and HEMA-Br. After the grafting of PSPMK brushes, the strong characteristic absorption peaks of S═O in SO_3^- groups appear at 1191 and 1039 cm^{-1}, which corroborate the existence of PSPMK in SB-*g*-NBrMGs.[44,45]

Furthermore, the thermal stability of SB-*g*-NBrMGs was evaluated by TGA in air atmosphere. As shown in Figure 1c, the thermo-decomposition temperature of the microgels is ca. 280.8 °C, indicating a good thermodynamic stability. Importantly, the thermo-decomposition temperature is much higher than the boiling point of water 100 °C, implying that the microgels have no thermal decomposition problem in the process of aqueous lubrication.

3.2. Morphology Characterization. The morphology of NBrMGs and SB-*g*-NBrMGs was investigated using the field-emission scanning electron microscopy (FE-SEM). As shown in Figure 2a, the NBrMGs colloidal particles formed homogeneously by the emulsifier-free emulsion polymerization, and had a mean diameter of ca. 292 nm. Through the EDXS spectrum in Figure 2c, the appearance of Br signal showed that HEMA-Br monomers were successfully copolymerized with NIPAAm, indicating a good immobilization of initiator ATRP-Br.

Afterward, the NBrMGs were functionalized with PSPMK brushes through the surface-initiated atom transfer radical polymerization. As revealed in Figure 2b, the size of the resulting modified microgels (ca. 576 nm) had an obvious increase in comparison with that of PNIPAAm-Br microgels. From the EDXS spectrum in Figure 2d, the new appearance of S and K signals indirectly verified the successful grafting of PSPMK brushes on NBrMGs. SEM images and EDXS spectra suggested a successful preparation of SB-*g*-NBrMGs intuitively.

Interestingly, the polymer brushes grafted microgels exhibited a fancy straw hat-shaped feature, which was attributed

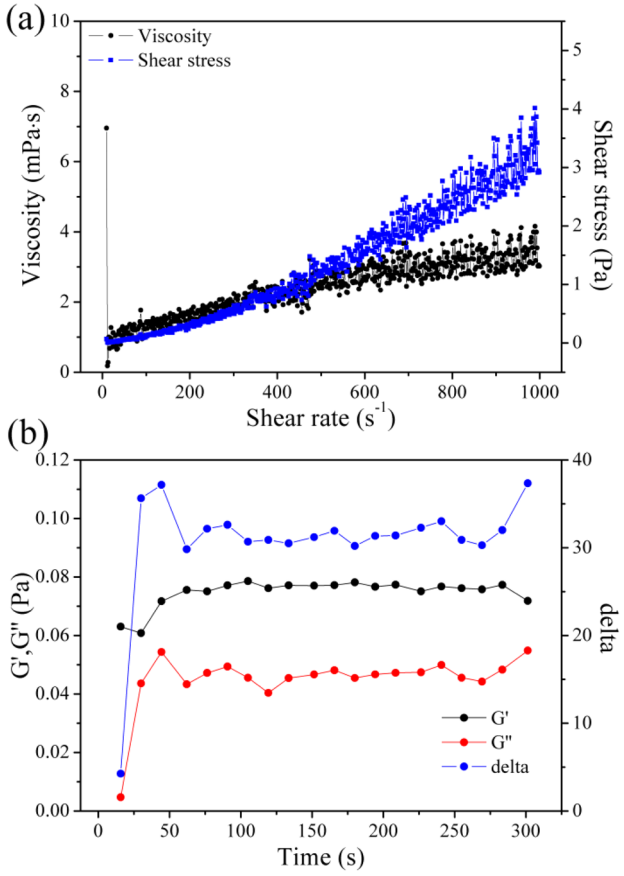

Figure 4. (a) Viscosity versus shear rate curves of SB-*g*-NBrMGs suspension (1.0 wt %). (b) Storage moduli (G'), loss moduli (G''), and delta of SB-*g*-NBrMGs suspension (1.0 wt %) as a function of time.

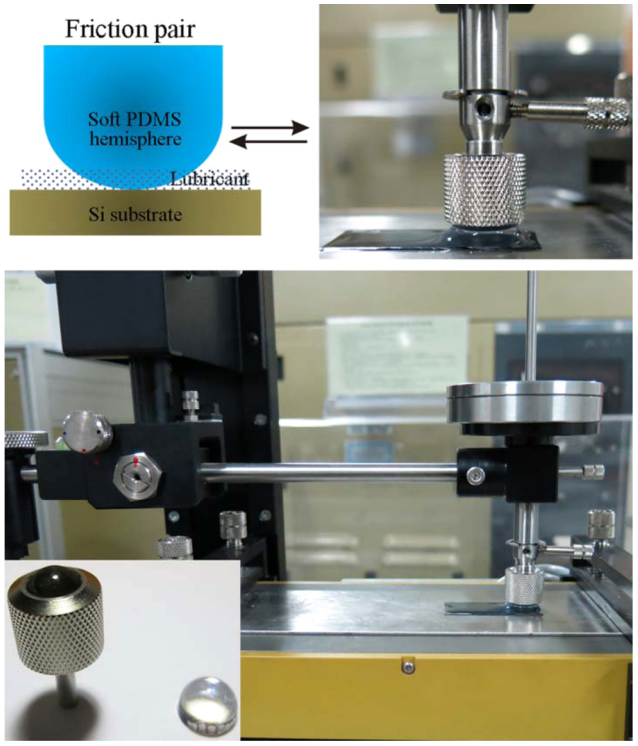

Figure 5. Schematic diagram illustrated the modified friction pairs, and the inset displayed the elastic PDMS hemisphere instead of traditional steel ball.

to the collapse of the colloid particles in dry state. Because of the uniform distribution of ATRP-Br in the PNIPAAm microgels, the PSPMK brushes were simultaneously grafted in the external and internal of microgels. This in turn shows that polymer bushes stretched the polymeric network of microgels. Thus, the grafted microgels show a plump sphere because of a water-filled polymer brushes in aqueous media. But after drying, a collapse occurred due to the dehydration of PSPMK brushes.

3.3. Particle Size and ζ-Potential in Aqueous Media. The hydrodynamic diameter and ζ-potential distributions of SB-*g*-NBrMGs in aqueous media were measured by using dynamic light scattering. As shown in Figure 3a, the hydrodynamic diameter of NBrMGs decreased from ca. 968 nm to ca. 627 nm as the temperature was increased from 25 to 50 °C, with the most drastic decrease occurring at the (volume phase transition temperature, VPTT) of ca. 36.4 °C. That is, after the grafting of PSPMK brushes, the SB-*g*-NBrMGs still maintained a good thermosensitive performance. In comparison with pure PNIPAAm microgels (32 °C), the VPTT of the modified microgels shifted to a higher temperature, which derived from the hydrophilic PSPMK grafted chains.[46,47] The calculated swelling ratio of SB-*g*-NBrMGs was 3.68, which was a key parameter for thermosensitive microgels. In addition, the particle dispersion index was about 0.2, and had no obvious change during the entire heating process, suggesting a narrow size distribution of SB-*g*-NBrMGs in aqueous media.

Importantly, as shown in Figure 3b, the ζ-potential of SB-*g*-NBrMGs showed a single peak with the value of −52.3 mv, indicating that the obtained hairy microgels were negatively charged. This charged modification originated from the coverage of negatively charged PSPMK brushes.[48−51] Due to the hydration mechanism, the polar charged group was a key factor to the formation of hydrated layer. The polyelectrolyte PSPMK brushes may play a hydration role in aqueous lubrication. The measurement of ζ-potential offered a precondition to the subsequent friction study.

3.4. Rheological Characterization. To evaluate the microgels as synthetic aqueous lubricants, we first assessed their rheological properties in aqueous media. Figure 4a showed the rheological curves of SB-*g*-NBrMGs suspensions (1.0 wt %). It is clear that the viscosity increased gradually with the increasing shear rate, indicating that the modified microgel suspensions can be classified as the shear-thickening type of the non-Newtonian fluid. To our best knowledge, the rheological behaviors of the pure PNIPAAm microgel suspension have been extensively investigated, and this type of microgels showed a characteristic shear-thinning phenomenon.[52−54] As for tribological application, the shear-thickening type of fluid was preferred. That is, the design of SB-*g*-NBrMGs was a positive improvement for lubrication. Shear-thickening fluids certainly entertain and spark our curiosity. According to the previous study,[51,55] the addition of a polymer "brush" grafted or adsorbed onto the particles' surface can prevent particles from getting close together. As for SB-*g*-NBrMGs suspension, the grafted PSPMK brushes widened the spatial distance between the microgels. With the increased shear rate, the PSPMK brushes were stretched to a higher degree, thereby leading to the destruction of the closely packed colloidal arrangement. That is, a more loose colloidal arrangement was formed on a microlevel, and the hairy microgel suspension exhibited a shear-thickening nature on a macro-level.

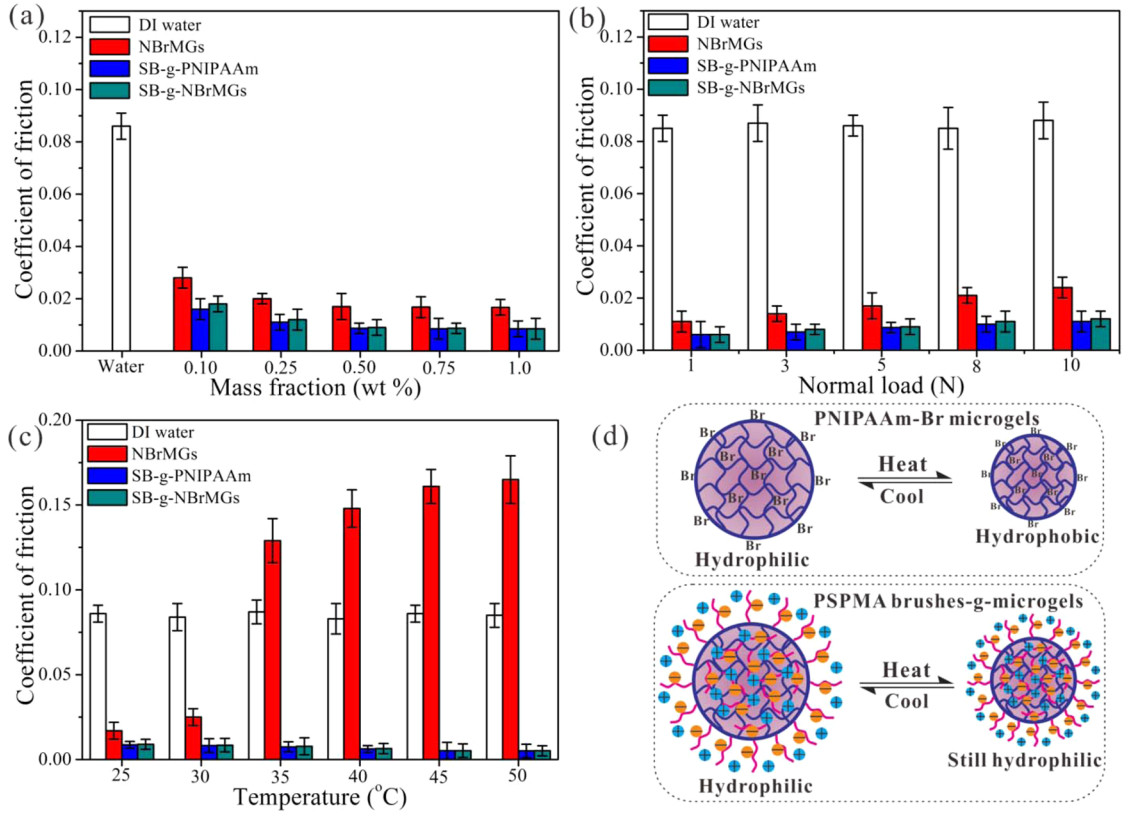

Figure 6. (a) COFs with NBrMGs, SB-*g*-PNIPAAm, and SB-*g*-NBrMGs suspensions with different concentrations under the normal load of 5 N at 25 °C. (b) COFs with NBrMGs, SB-*g*-PNIPAAm, and SB-*g*-NBrMGs suspensions (0.5 wt %) under different normal loads. (c) COFs with NBrMGs, SB-*g*-PNIPAAm, and SB-*g*-NBrMGs suspensions (0.5 wt %) under the normal load of 5 N at different temperature. (d) Schematic diagram illustrating the hydrophilicity/hydrophobicity transition of NBrMGs and SB-*g*-NBrMGs around the VPTT. The deionized water was used as a reference.

Figure 4b showed the plots of storage moduli (G'), loss moduli (G''), and delta of SB-*g*-NBrMGs suspensions (1.0 wt %) as a function of time. It is evident that the storage modulus (about 0.077 Pa) was higher than the loss modulus (about 0.047 Pa) for SB-*g*-NBrMGs suspension, indicating that the sample behaved as a viscoelastic solid under the shear stress. During the entire shear process, the G' and G'' were stable, indicating a colloidal stability. In addition, the delta of SB-*g*-NBrMGs suspension was 26.8, suggesting a certain capability of dispersing energy away from the load-bearing surfaces. In short, using the SB-*g*-NBrMGs suspension as aqueous lubricant, the shear-thickening property and the increased delta value were beneficial for aqueous lubrication.

3.5. Tribological Property. To elucidate the effect of charged polymer brushes on aqueous lubrication, the tribological property of SB-*g*-NBrMGs was investigated in comparison with PNIPAAm microgels and brush-like polymer SB-*g*-PNIPAAm. Because the articular cartilage is soft and elastic, the friction pairs comprising a soft PDMS hemisphere and a silicon wafer were employed to study the aqueous lubrication of SB-*g*-NBrMGs. The modified friction device is shown in Figure 5, and the inset displayed the elastic PDMS hemisphere instead of traditional steel ball.

Figure 6a showed the coefficient of friction (COF) of NBrMGs, SB-*g*-PNIPAAm, and SB-*g*-NBrMGs with different concentrations under the normal load of 5 N at 25 °C. It is clear that the COF of SB-*g*-NBrMGs was lower than that of NBrMGs, and had no obvious difference with that of SB-*g*-PNIPAAm. With increasing the normal load, the COF of SB-*g*-NBrMGs had a gradual increase, and the variation trend was the same as the NBrMGs and SB-*g*-PNIPAAm, which was attributed to the deformation of soft matter under pressure. Since the viscosity of SB-*g*-NBrMGs suspension was higher than that of pure water, the COF of SB-*g*-NBrMGs was lower than that of pure water. In addition, SB-*g*-NBrMGs can be adsorbed onto the surface of friction pairs to form compact adsorbed film. At a high concentration, the adsorption would reach saturation, so the COF did not show an obvious increase finally. In Figure 7a and b, after friction, the XPS spectra of adsorption layer on silicon wafer verified the adsorption of SB-*g*-NBrMGs on the friction pair. Differently, the COF lubricated by PNIPAAm microgel suspension had a marked increase with the increased temperature, especially around the VPTT, while the lubrication system using the SB-*g*-NBrMGs or SB-*g*-PNIPAAm showed a gradually decreasing coefficient of friction with the increased temperature.

Obviously, SB-*g*-NBrMGs microgels, as an aqueous lubricant additive, present a more desirable tribological property than traditional PNIPAAm microgels, and also achieve the low friction such as the brush-like polyelectrolyte SB-*g*-PNIPAAm. Using the polyelectrolyte hairy microgels as a lubricant, the COF for the soft friction pair were in the range of 0.005−0.015 under normal loads (Figure 6b), which have achieved the category of articular cartilage lubrication (COF = 0.001−0.03).

From the perspective of lubrication mechanism, the lubrication using the SB-*g*-NBrMGs was strongly related to the mechanism of hydration lubrication. Because of the reluctance of the hydration layer to be squeezed out, the

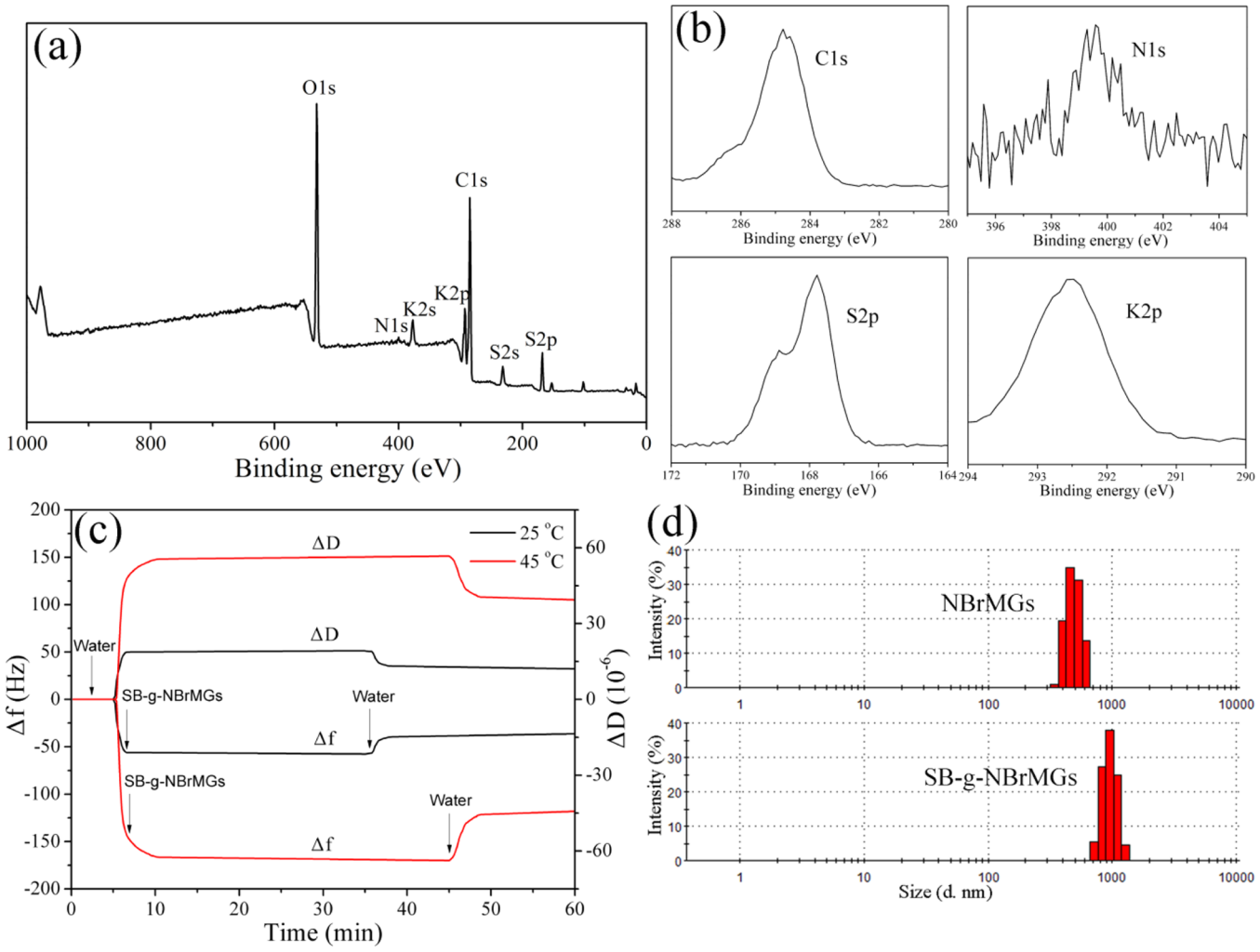

Figure 7. (a) XPS spectra of adsorption layer on silicon wafer lubricated by SB-*g*-NBrMGs suspensions. (b) XPS C 1s, N 1s, S 2p, and K 2p spectra of adsorption layer with SB-*g*-NBrMGs suspensions. (c) Plots for the time dependence of the resonant frequency shift (Δf) and corresponding dissipation (ΔD) of the QCM-D after the addition of SB-*g*-NBrMGs suspension (0.1 wt %). (d) Hydrodynamic size distribution of microgels in aqueous media after friction test.

hydrated layer around the charged polymer brushes can sustain a large normal pressure, but under shear this hydration layer shows a fluid property because of the rapid relaxation.[56] After the grafting of polymer brushes, the steric factor also contributes to the good lubrication effect.[29,57] That is, mutually compressed polymer brushes in aqueous media resist interpenetration, because of the excluded-volume effect arising from chain configurational entropy. Particularly, for the polyelectrolyte brushes, this excluded-volume effect is enhanced by the large osmotic pressure exerted by mobile counterions within the brushes.[18] For SB-*g*-NBrMGs microgels, the hydrated layer surrounding the charged hairy microgels reduces the self-energy of the enclosed charge, and it is difficult to permanently remove a water molecule from the hydration sheath because of a large emerge of dehydration. Thus, the hydration lubrication and the excluded-volume effect can be achieved by hydrophilic charged PSPMK brushes. In short, the hydrophobicity and surface charge were two key elements for the formation of hydrated layer, which played a decisive role for hydration lubrication. Therefore, the hydrophobicity and surface charge were two main factors influencing the COF in aqueous lubrication.

In tribology, the temperature was an important factor for the friction change. When the temperature was increased above the VPTT, the thermal breakage of the hydrogen bonds enabled the hydrophobicity of PNIPAAm chains, which weakened the hydration lubrication of NBrMGs microgels illustrated in Figure 6d. Thus, for NBrMGs suspension, there was an obvious transition of coefficient of friction around the VPTT, and the coefficient of friction become large with the temperature. This increased coefficient of friction was undesirable if used in joint aqueous lubrication. However, for SB-*g*-NBrMGs suspension, the charged polymer brushes enabled a good hydrophilicity of the outer layer of SB-*g*-NBrMGs in spite of phase transition above the VPTT (Figure 6d). In this case, the hydrated layer still existed around the microgels, which effectively protected the hydration lubrication. This interesting phenomenon not only enabled the consistent good lubricating effect with the temperature but also provided volume phase transition for thermoresponsive application in controlled drug release. Under the human environment, using the conventional PNIPAAm microgels as a lubricant will cause an undesirable lubricity, whereas the polyelectrolyte brushes modified microgels will overcome the shortcoming.

In addition to continuous hydrophilicity, the enhanced interfacial adsorption triggered by the elevated temperature also contributes to the ultralow and gradually decreasing coefficient

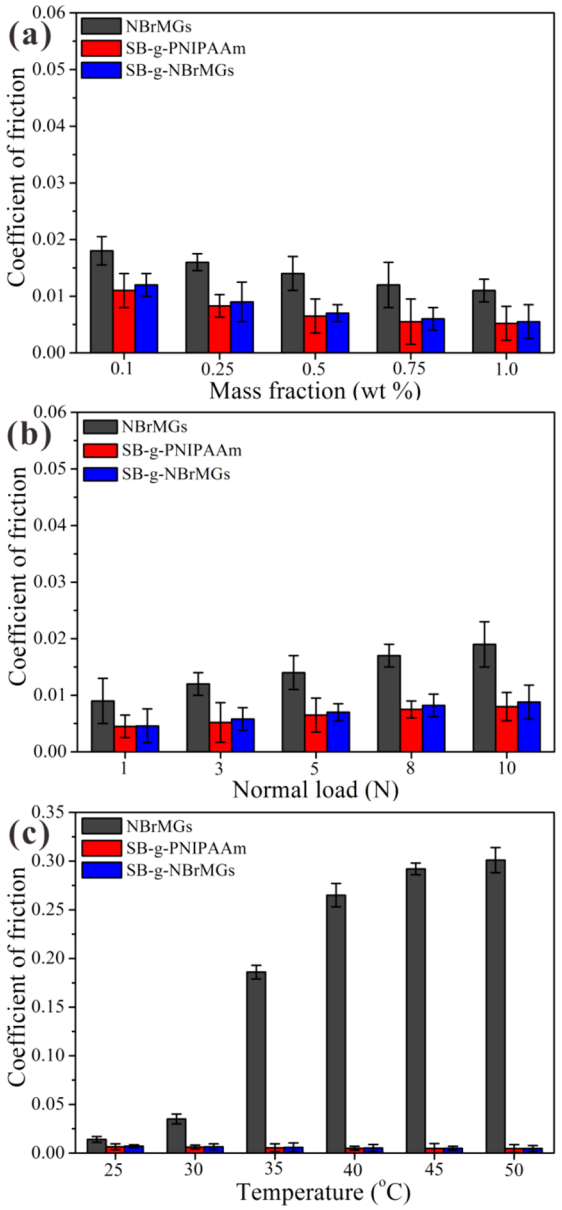

Figure 8. (a) COFs with NBrMGs, SB-*g*-PNIPAAm and SB-*g*-NBrMGs suspensions with different concentrations using the modified PDMS hemisphere under the normal load of 5 N at 25 °C. (b) COFs with NBrMGs, SB-*g*-PNIPAAm, and SB-*g*-NBrMGs suspensions (0.5 wt %) under different normal loads using the modified PDMS hemisphere. (c) COFs with NBrMGs, SB-*g*-PNIPAAm, and SB-*g*-NBrMGs suspensions (0.5 wt %) using the modified PDMS hemisphere under the normal load of 5 N at different temperature.

of friction of SB-*g*-NBrMGs aqueous suspension. As shown in Figure 7c, the physisorption of SB-*g*-NBrMGs in the swollen and collapsed states on the friction pair was investigated by a quartz crystal microbalance with dissipation (QCM-D). After the addition of SB-*g*-NBrMGs aqueous suspension, the Δf decreased significantly and the corresponding ΔD had an obvious increase, suggesting a marked physisorption on the friction pair. Notably, it is clear that the Δf at 45 °C (in collapse state) was much larger than that at 25 °C (in swollen state). The VPT caused by the increasing temperature led to the collapse of microgels, suggesting a more compact arrangement of microgels on the substrate, even a multilayer adsorption.[58,59] Thus, the higher temperature caused the increase of density of

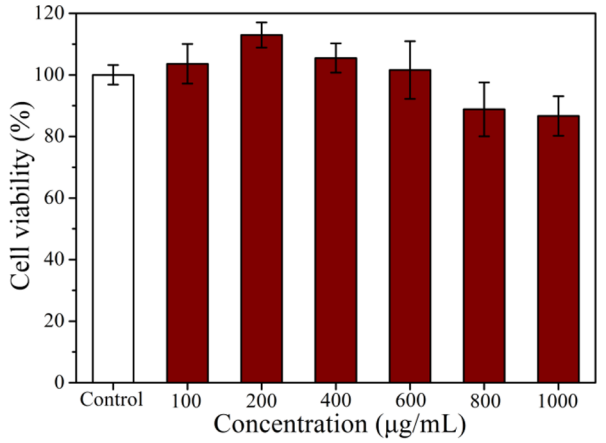

Figure 9. Cell viability of Hela cells incubated with different concentrations of SB-*g*-NBrMGs.

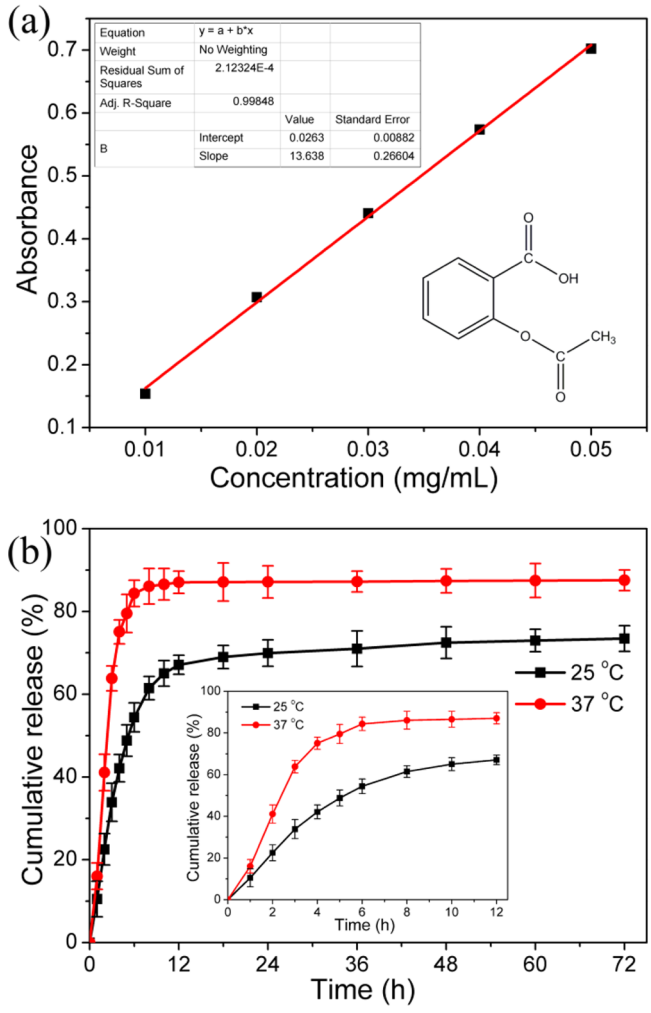

Figure 10. (a) The calibration curve of aspirin drawn based on the UV absorption. (b) The release profiles of aspirin-SB-*g*-NBrMGs within 72 h in PBS buffer solutions (pH = 7.4) at 25 and 37 °C. The release profiles within 12 h were in the inset.

the microgels attached to the surface. For SB-*g*-NBrMGs, the adsorbed film was still hydrophilic, which in turn improved both boundary lubrication and hydration lubrication.[26] For NBrMGs, the adsorbed film changed from hydrophilic to hydrophobic, and the hydration lubrication was weakened.

dx.doi.org/10.1021/am506026e | ACS Appl. Mater. Interfaces 2014, 6, 20452−20463

From this view, the grafting of charged polymer brushes on the microgels showed a significant promoting role for hydration lubrication. In addition, the wear of microgels was investigated by DLS. Figure 7d shows the size distribution of NBrMGs and SB-*g*-NBrMGs after the friction test. It is found that no new peaks appeared in the size distribution map after the friction tests, revealing that no microgel colloids were broken up in the friction process. This indicated that microgel structures are capable of undergoing a certain deformation in responsive to environmental change. In short, compared with pure thermosensitive microgels, the polyelectrolyte brushes grafted thermoresponsive microgels can maintain a good lubricating effect at a higher temperature. Compared with brush-like polyelectrolyte, the polyelectrolyte brushes grafted thermoresponsive microgels have a temperature- triggered drug release, which have been confirmed in Figure 10.

In order to mimic the lubricating environment of synovial fluid, the PDMS hemisphere was coated with PSPMK brushes or PNIPAAm hydrogel. The coefficient of friction with the modified PDMS hemisphere is shown in Figure 8. It is clear that the coefficient of friction using the modified PDMS hemisphere at different concentrations (Figure 8a) or under different normal load (Figure 8b) was lower than that using the pure PDMS hemisphere, which was attributed to hydrophilic modification of friction contact. As for chain structure, the SB-*g*-PNIPAAm polymer showed a brush-like architecture with PNIPAAm chains as the backbone and PSPMK brushes as the branched chains. That is, the component exposed to the outside was PSPMK brushes. For SB-*g*-NBrMGs microgels, PSPMK brushes were also exposed to the outside. The lubricating effect depended on the hydration lubrication of PSPMK brushes, thereby leading to no obvious difference in the COFs between these two structures. This comparison was used to illustrate that the hairy microgels had the same good lubricating effect as the traditional biomimetic brush-like polymer. Notably, in Figure 8c, the COF of NBrMGs had a more dramatic increase with the temperature than that using pure PDMS hemisphere. At a higher temperature, the jointly hydrophobic transition of NBrMGs and PNIPAAm hydrogel shell on the PDMS led to a higher friction coefficient. This result demonstrated that the lubricating effect of the SB-*g*-NBrMGs was superior to NBrMGs and the biomimetic modification of PDMS hemisphere was more suitable for SB-*g*-NBrMGs.

3.6. In Vitro Cytotoxicity. As a biomimetic lubricating material, nontoxicity or low toxicity is a key parameter for biomedical applications. Cell viability assays were performed to investigate the cytotoxicity of SB-*g*-NBrMGs. Hela cells were incubated with different concentration of the hairy microgels for 24 h. As shown in Figure 9, the cell viability remained over 85% in the range of 100−1000 μg/mL, indicating that the SB-*g*-NBrMGs exhibited good biocompatibility for Hela cells. This result demonstrated that the modified microgels had a large potential for clinical applications.

3.7. In Vitro Drug Loading and Release. For SB-*g*-NBrMGs as a biomimetic synthetic synovial fluid, except for a good aqueous lubricating effect, the drug therapy was also desirable in the arthritis treatment.[60,61] In our work, in vitro drug loading and release using SB-*g*-NBrMGs as a carrier was studied at 25 and 37 °C. Aspirin, as a specific drug for arthritis, was chosen as the model drug. Since the network structure of inner microgel cores and the interspace among outer PSPMK brushes can both accommodate the aspirin, SB-*g*-NBrMGs can serve as drug carriers to load the aspirin. The calibration curve and chemical structure of aspirin were displayed in Figure 10a. Through calculation, LC and EE were 31.6% and 46.2%, respectively, which demonstrated that the SB-*g*-NBrMGs had a good drug loading capacity and can be used as a drug carrier.

To illustrate whether the grafting of PSPMK brushes affected the thermoresponsive drug release performance, the drug release profiles of aspirin-SB-*g*-NBrMGs delivery systems in PBS buffer solution (pH = 7.4) are shown in Figure 10b, which clearly indicated that there was obvious difference between drug-release rates at different temperature. At 25 °C, 67.1% and 73.4% of aspirin were released within 12 and 72 h, respectively. At 37 °C, 87.1% and 87.5% of aspirin were released within 12 and 72 h, respectively, suggesting an obvious increase in drug-release rate. In the inset (Figure 10b), the drug-release system at 25 °C showed a slow and sustained release of aspirin, and the system at 37 °C displayed a burst-release effect within the initial 6 h. This demonstrated that SB-*g*-NBrMGs still possess an intelligent thermoresponsive performance for drug release system the same as pure PNIPAAm microgels.

The drug release triggered by a high temperature can be applicable when an immediate high dosage is required, for instance, for an acute infection or inflammation. The intelligent drug release, compatible with low-friction performance, may achieve simultaneous cartilage lubrication and arthritis treatment.

4. CONCLUSION

A potential biomimetic synovial fluid was demonstrated based on PSPMK brushes grafted PNIPAAm microgels, capable of outstanding hydration lubrication together with temperature-triggered drug release performance. A good lubricating effect was achieved through hydration mechanism of charged PSPMK brushes, while the PNIPAAm cores endowed the soft hairy microgels with a temperature-triggered drug release performance. The hairy charged polymer brushes grafted thermosensitive microgels design offers immense potentials as intelligent synovial fluid for high-efficiency joint lubrication, together with possible arthritis treatment in clinical medicine.

AUTHOR INFORMATION

Corresponding Authors

*E-mail: wangxl@licp.cas.cn.

*E-mail: zhouf@licp.cas.cn.

Notes

The authors declare no competing financial interest.

ACKNOWLEDGMENTS

This work was financially supported by NSFC (21125316, 21303233, 51335010, 21434009), 973 projects (2013CB632300), and Key Research Program of CAS (KJZD-EW-M01).

REFERENCES

(1) Gong, J. P. Friction and Lubrication of Hydrogels? Its Richness and Complexity. *Soft Matter* **2006**, *2*, 544−552.

(2) Neu, C. P.; Komvopoulos, K.; Reddi, A. H. The Interface of Functional Biotribology and Regenerative Medicine in Synovial Joints. *Tissue Eng., Part B* **2008**, *14*, 235−247.

(3) Klein, J. Repair or Replacement—A Joint Perspective. *Science* **2009**, *323*, 47−48.

(4) Waller, K. A.; Zhang, L. X.; Elsaid, K. A.; Fleming, B. C.; Warman, M. L.; Jay, G. D. Role of Lubricin and Boundary Lubrication

in the Prevention of Chondrocyte Apoptosis. *Proc. Natl. Acad. Sci. U.S.A.* **2013**, *110*, 5852−5857.
(5) Kisiday, J.; Jin, M.; Kurz, B.; Hung, H.; Semino, C.; Zhang, S.; Grodzinsky, A. J. Self-Assembling Peptide Hydrogel Fosters Chondrocyte Extracellular Matrix Production and Cell Division: Implications for Cartilage Tissue Repair. *Proc. Natl. Acad. Sci. U.S.A.* **2002**, *99*, 9996−10001.
(6) Wathier, M.; Lakin, B. A.; Bansal, P. N.; Stoddart, S. S.; Snyder, B. D.; Grinstaff, M. W. A Large-Molecular-Weight Polyanion, Synthesized via Ring-Opening Metathesis Polymerization, as a Lubricant for Human Articular Cartilage. *J. Am. Chem. Soc.* **2013**, *135*, 4930−4933.
(7) Sivan, S.; Schroeder, A.; Verberne, G.; Merkher, Y.; Diminsky, D.; Priev, A.; Maroudas, A.; Halperin, G.; Nitzan, D.; Etsion, I.; Barenholz, Y. Liposomes Act as Effective Biolubricants for Friction Reduction in Human Synovial Joints. *Langmuir* **2010**, *26*, 1107−1116.
(8) Verberne, G.; Schroeder, A.; Halperin, G.; Barenholz, Y.; Etsion, I. Liposomes as Potential Biolubricant Additives for Wear Reduction in Human Synovial Joints. *Wear* **2010**, *268*, 1037−1042.
(9) Yasuda, K.; Ping Gong, J.; Katsuyama, Y.; Nakayama, A.; Tanabe, Y.; Kondo, E.; Ueno, M.; Osada, Y. Biomechanical Properties of High-Toughness Double Network Hydrogels. *Biomaterials* **2005**, *26*, 4468−4475.
(10) Kim, I. L.; Mauck, R. L.; Burdick, J. A. Hydrogel Design for Cartilage Tissue Engineering: A Case Study with Hyaluronic Acid. *Biomaterials* **2011**, *32*, 8771−8782.
(11) Pan, Y.-S.; Xiong, D.-S.; Ma, R.-Y. A Study on the Friction Properties of Poly(vinyl alcohol) Hydrogel as Articular Cartilage against Titanium Alloy. *Wear* **2007**, *262*, 1021−1025.
(12) Noguchi, T.; Yamamuro, T.; Oka, M.; Kumar, P.; Kotourayt, Y.; Hyonyt, S.; Ikada, Y. Poly(vinyl alcohol) Hydrogel as an Artificial Articular Cartilage: Evaluation of Biocompatibility. *J. Appl. Biomater.* **1991**, *2*, 101−107.
(13) Fisher, J. P.; Jo, S.; Mikos, A. G.; Reddi, A. H. Thermoreversible Hydrogel Scaffolds for Articular Cartilage Engineering. *J. Biomed. Mater. Res., Part A* **2004**, *71*, 268−274.
(14) Klein, J. Hydration Lubrication. *Friction* **2013**, *1*, 1−23.
(15) Lee, S.; Spencer, N. D. Sweet, Hairy, Soft, and Slippery. *Science* **2008**, *319*, 575−576.
(16) Banquy, X.; Burdynska, J.; Lee, D. W.; Matyjaszewski, K.; Israelachvili, J. Bioinspired Bottle-Brush Polymer Exhibits Low Friction and Amontons-Like Behavior. *J. Am. Chem. Soc.* **2014**, *136*, 6199−6202.
(17) Raviv, U.; Laurat, P.; Klein, J. Fluidity of Water Confined to Subnanometer films. *Nature* **2001**, *413*, 51−54.
(18) Raviv, U.; Giasson, S.; Kampf, N.; Gohy, J.-F.; Jerome, R.; Klein, J. Lubrication by Charged Polymers. *Nature* **2003**, *425*, 163−165.
(19) Liu, G.; Zhu, C.; Xu, J.; Xin, Y.; Yang, T.; Li, J.; Shi, L.; Guo, Z.; Liu, W. Thermo-Responsive Hollow Silica Microgels with Controlled Drug Release Properties. *Colloids Surf., B* **2013**, *111C*, 7−14.
(20) Islam, M. R.; Li, X.; Smyth, K.; Serpe, M. J. Polymer-Based Muscle Expansion and Contraction. *Angew. Chem., Int. Ed.* **2013**, *52*, 10330−10333.
(21) Li, X.; Serpe, M. J. Understanding and Controlling the Self-Folding Behavior of Poly(N-Isopropylacrylamide) Microgel-Based Devices. *Adv. Funct. Mater.* **2014**, *24*, 4119−4126.
(22) Kwon, H. J.; Gong, J. P. Negatively Charged Polyelectrolyte Gels as Bio-Tissue Model System and for Biomedical Application. *Curr. Opin. Colloid Interface Sci.* **2006**, *11*, 345−350.
(23) Lyon, L. A.; Meng, Z.; Singh, N.; Sorrell, C. D.; St John, A. Thermoresponsive Microgel-Based Materials. *Chem. Soc. Rev.* **2009**, *38*, 865−874.
(24) Liu, G.; Li, X.; Xiong, S.; Li, L.; Chu, P. K.; Yeung, K. W. K.; Wu, S.; Xu, Z. Fluorine-Containing pH-Responsive Core/Shell Microgel Particles: Preparation, Characterization, and Their Applications in Controlled Drug Release. *Colloid Polym. Sci.* **2011**, *290*, 349−357.
(25) Zakrevskyy, Y.; Richter, M.; Zakrevska, S.; Lomadze, N.; Klitzing, R. v.; Santer, S. Light-Controlled Reversible Manipulation of Microgel Particle Size Using Azobenzene-Containing Surfactant. *Adv. Funct. Mater.* **2012**, *22*, 5000−5009.
(26) Liu, G.; Wang, X.; Zhou, F.; Liu, W. Tuning the Tribological Property with Thermal Sensitive Microgels for Aqueous Lubrication. *ACS. Appl. Mater. Interfaces* **2013**, *5*, 10842−10852.
(27) de Vicente, J.; Stokes, J. R.; Spikes, H. A. Soft Lubrication of Model Hydrocolloids. *Food Hydrocolloids* **2006**, *20*, 483−491.
(28) Dėdinaitė, A. Biomimetic Lubrication. *Soft Matter* **2012**, *8*, 273−284.
(29) Ohsedo, Y.; Takashina, R.; Gong, J. P.; Osada, Y. Surface Friction of Hydrogels with Well-Defined Polyelectrolyte Brushes. *Langmuir* **2004**, *20*, 6549−6555.
(30) Klein, J.; Kumacheva, E.; Mahalu, D.; Perahia, D.; Fetters, L. J. Reduction of Frictional Forces between Solid Surfaces Bearing Polymer Brushes. *Nature* **1994**, *370*, 634−636.
(31) Moffitt, M. G. Self-Assembly of Polymer Brush-Functionalized Inorganic Nanoparticles: From Hairy Balls to Smart Molecular Mimics. *J. Phys. Chem. Lett.* **2013**, *4*, 3654−3666.
(32) Zhao, L.; Qin, H.; Hu, Z.; Zhang, Y.; Wu, R.; Zou, H. A Poly(ethylene glycol)-Brush Decorated Magnetic Polymer for Highly Specific Enrichment of Phosphopeptides. *Chem. Sci.* **2012**, *3*, 2828−2838.
(33) Wei, Q.; Cai, M.; Zhou, F.; Liu, W. Dramatically Tuning Friction Using Responsive Polyelectrolyte Brushes. *Macromolecules* **2013**, *46*, 9368−9379.
(34) South, A. B.; Lyon, L. A. Autonomic Self-Healing of Hydrogel Thin Films. *Angew. Chem., Int. Ed.* **2010**, *49*, 767−771.
(35) Gong, X.; Peng, S.; Wen, W.; Sheng, P.; Li, W. Design and Fabrication of Magnetically Functionalized Core/Shell Microspheres for Smart Drug Delivery. *Adv. Funct. Mater.* **2009**, *19*, 292−297.
(36) Patnaik, S.; Sharma, A. K.; Garg, B. S.; Gandhi, R. P.; Gupta, K. C. Photoregulation of Drug Release in Azo-Dextran Nanogels. *Int. J. Pharm.* **2007**, *342*, 184−193.
(37) Li, B.; Yu, B.; Huck, W. T.; Zhou, F.; Liu, W. Electrochemically Induced Surface-Initiated Atom-Transfer Radical Polymerization. *Angew. Chem., Int. Ed.* **2012**, *124*, 5182−5185.
(38) Yan, J.; Li, B.; Yu, B.; Huck, W. T.; Liu, W.; Zhou, F. Controlled Polymer-Brush Growth from Microliter Volumes Using Sacrificial-Anode Atom-Transfer Radical Polymerization. *Angew. Chem., Int. Ed.* **2013**, *52*, 9125−9129.
(39) Raviv, U.; Giasson, S.; Kampf, N.; Gohy, J.-F.; Jerome, R.; Klein, J. Normal and Frictional Forces between Surfaces Bearing Polyelectrolyte Brushes. *Langmuir* **2008**, *24*, 8678−8687.
(40) Setton, L. Polymer Therapeutics: Reservoir Drugs. *Nat. Mater.* **2008**, *7*, 172−174.
(41) Wang, X.; Ye, Q.; Gao, T.; Liu, J.; Zhou, F. Self-Assembly of Catecholic Macroinitiator on Various Substrates and Surface-Initiated Polymerization. *Langmuir* **2012**, *28*, 2574−2581.
(42) Matyjaszewski, K.; Gaynor, S. G. Preparation of Hyperbranched Polyacrylates by Atom Transfer Radical Polymerization. 2. Kinetics and Mechanism of Chain Growth for the Self-Condensing Vinyl Polymerization of 2-((2-Bromopropionyl)oxy)ethyl Acrylate. *Macromolecules* **1997**, *30*, 7034−7041.
(43) Matyjaszewski, K.; Gaynor, S. G.; Kulfan, A.; Podwika, M. Preparation of Hyperbranched Polyacrylates by Atom Transfer Radical Polymerization. 1. Acrylic Ab* Monomers in ″Living″ Radical Polymerizations. *Macromolecules* **1997**, *30*, 5192−5194.
(44) Ramstedt, M.; Cheng, N.; Azzaroni, O.; Mossialos, D.; Mathieu, H. J.; Huck, W. T. S. Synthesis and Characterization of Poly(3-sulfopropylmethacrylate) Brushes for Potential Antibacterial Applications. *Langmuir* **2007**, *23*, 3314−3321.
(45) Vo, C.-D.; Schmid, A.; Armes, S. P. Surface Atrp of Hydrophilic Monomers from Ultrafine Aqueous Silica Sols Using Anionic Polyelectrolytic Macroinitiators. *Langmuir* **2007**, *23*, 408−413.
(46) Park, J.-S.; Kataoka, K. Precise Control of Lower Critical Solution Temperature of Thermosensitive Poly(2-isopropyl-2-oxazoline) via Gradient Copolymerization with 2-Ethyl-2-oxazoline as a Hydrophilic Comonomer. *Macromolecules* **2006**, *39*, 6622−6630.

(47) Koga, S.; Sasaki, S.; Maeda, H. Effect of Hydrophobic Substances on the Volume-Phase Transition of N-Isopropylacrylamide Gels. *J. Phys. Chem. B* **2001**, *105*, 4105−4110.
(48) Irigoyen, J.; Arekalyan, V. B.; Navoyan, Z.; Iturri, J.; Moya, S. E.; Donath, E. Spherical Polyelectrolyte Brushes' Constant ζ-Potential with Varying Ionic Strength: An Electrophoretic Study Using a Hairy Layer Approach. *Soft Matter* **2013**, *9*, 11609−11617.
(49) Zhao, Y.-H.; Zhu, X.-Y.; Wee, K.-H.; Bai, R. Achieving Highly Effective Non-Biofouling Performance for Polypropylene Membranes Modified by UV-Induced Surface Graft Polymerization of Two Oppositely Charged Monomers. *J. Phys. Chem. B* **2010**, *114*, 2422−2429.
(50) Liu, G.; Cai, M.; Wang, X.; Zhou, F.; Liu, W. Core−Shell-Corona-Structured Polyelectrolyte Brushes-Grafting Magnetic Nanoparticles for Water Harvesting. *ACS Appl. Mater. Interfaces* **2014**, *6*, 11625−11632.
(51) Liu, G.; Cai, M.; Zhou, F.; Liu, W. Charged Polymer Brushes-Grafted Hollow Silica Nanoparticles as a Novel Promising Material for Simultaneous Joint Lubrication and Treatment. *J. Phys. Chem. B* **2014**, *118*, 4920−4931.
(52) Berndt, I.; Richtering, W. Doubly Temperature Sensitive Core−Shell Microgels. *Macromolecules* **2003**, *36*, 8780−8785.
(53) Senff, H.; Richtering, W. Rheology of a Temperature Sensitive Core−Shell Latex. *Langmuir* **1999**, *15*, 102−106.
(54) Stieger, M.; Pedersen, J. S.; Lindner, P.; Richtering, W. Are Thermoresponsive Microgels Model Systems for Concentrated Colloidal Suspensions? A Rheology and Small-Angle Neutron Scattering Study. *Langmuir* **2004**, *20*, 7283−7292.
(55) Wagner, N. J.; Brady, J. F. Shear Thickening in Colloidal Dispersions. *Phys. Today* **2009**, *62*, 27−32.
(56) Gaisinskaya, A.; Ma, L.; Silbert, G.; Sorkin, R.; Tairy, O.; Goldberg, R.; Kampf, N.; Klein, J. Hydration Lubrication: Exploring a New Paradigm. *Faraday Discuss.* **2012**, *156*, 217−233.
(57) Kobayashi, M.; Terada, M.; Takahara, A. Polyelectrolyte Brushes: A Novel Stable Lubrication System in Aqueous Conditions. *Faraday Discuss.* **2012**, *156*, 403−412.
(58) Liu, G.; Zhang, G. Collapse and Swelling of Thermally Sensitive Poly(N-isopropylacrylamide) Brushes Monitored with a Quartz Crystal Microbalance. *J. Phys. Chem. B* **2005**, *109*, 743−747.
(59) Wu, K.; Wu, B.; Wang, P.; Hou, Y.; Zhang, G.; Zhu, D.-M. Adsorption Isotherms and Dissipation of Adsorbed Poly(N-isopropylacrylamide) in Its Swelling and Collapsed States. *J. Phys. Chem. B* **2007**, *111*, 8723−8727.
(60) Gao, Y.; Zago, G. P.; Jia, Z.; Serpe, M. J. Controlled and Triggered Small Molecule Release from a Confined Polymer Film. *ACS Appl. Mater. Interfaces* **2013**, *5*, 9803−9808.
(61) Gao, Y.; Ahiabu, A.; Serpe, M. J. Controlled Drug Release from the Aggregation−Disaggregation Behavior of pH-Responsive Microgels. *ACS Appl. Mater. Interfaces* **2014**, *6*, 13749−13756.